Electronic Supplementary Material (ESI) for Nanoscale.

Supporting Information

A single-light triggered and dual-imaging guided multifunctional platform for combined photothermal and photodynamic therapy based on TD-controlled and indocyanine green-loaded CuS@mSiO$_2$

Qing You, Qi Sun, Jinping Wang, Xiaoxiao Tan, Xiaojuan Pang, Li Liu, Meng Yu， Fengping Tan, Nan Li*

Tianjin Key Laboratory of Drug Delivery & High-Efficiency, School of Pharmaceutical Science and Technology, Tianjin University, 300072 Tianjin, PR China

Corresponding author at: School of Pharmaceutical Science and Technology, Tianjin University, 300072, Tianjin, PR China.

Tel: +86-022-27404986

E-mail address: linan19850115@163.com

Calculation of the photothermal conversion efficiency

The photothermal conversion efficiency of CuS@mSiO$_2$-TD/ICG nanoparticles was measured according to the references 1. The CuS@mSiO$_2$-TD/ICG nanoparticles with the Cu@mSiO$_2$ concentration of 200 ug/mL and ICG 10 ug/mL underwent continuous irradiation of 808 nm laser (1.5 W/cm^2) until steady state temperature was reached. Then the laser was shut off, and the aqueous solution was naturally cooled to the environment temperature. The temperature change of the aqueous solution was recorded immediately (Fig. 4c). The η value was calculated as follows:

$$\eta = \frac{hS(Tmax - TSurr) - QS}{I\,(1 - 10 - A808)} \times 100\% \qquad (1)$$

here h is the heat transfer coefficient, S is the surface area of the container, and the value of hS is obtained from the Eq.4 and Figure S6b. The maximum steady temperature (T_{max}) and environmental temperature (T_{Surr}) were 58.8°C and 23.6°C, respectively. The laser power for irradiation was 1.5 W/cm^2. The absorbance of the CuS@mSiO$_2$-TD/ICG nanoparticles at 808 nm A_{808} was 1.306. Q_S was heat dissipated from the light absorbed by the solvent and container. A dimensionless parameter θ was calculated as followed:

$$\theta = \frac{T - TSurr}{Tmax - TSurr} \times 100\% \qquad (2)$$

A sample system time constant τ_s coul be calculated as Eq.3.

$$t = \tau_s \ln(\theta) \qquad (3)$$

According to Fig.4b, τ_s was determined and calculated to be 196.40 s.

$$hs = \frac{mD - CD}{\tau s} \times 100\% \quad (4)$$

In addition, m_D was 0.5 g and C_D was 4.2 J/g·°C. Thus, according to Eq.4., hS was calculated to be 10.69 mW/°C.

Qs was heat dissipated from the light absorbed by the container itself, which was determined independently to be 3.5 mW using a container containing pure water. Thus, substituting according values of each parameters to Eq.1, the 808 nm laser photothermal conversion efficiency (η) of the CuS@mSiO_2-TD/ICG nanoparticles could be calculated to be 26.2%.

$^1O_2$ quantum yields determination by chemical method

$^1O_2$ quantum yields determination was performed with a slightly modified version of chemical method using DPBF reported by Zhou Jiang et al [2]. Phthalocyanine zinc (ZnPc), whose $^1O_2$ quantum yield is 0.56 in DMF [3], was used as the reference. When the mixture of DPBF and free ICG was irradiated at 808 nm and the mixture of DPBF and ZnPc was irradiated at 670 nm for 10 min, respectively, the absorbance of the formulations at 410 nm were measured every 2 min for a 10 min period with an UV-visble spectrophotometer. The decreasing rate of DPBF absorption (K_{DPBF}) depended on the irradiation time interval following the first-order kinetics (Eq.1) [4, 5]. (t: irradiation time, A_0: absorbance at t= 0, A_t : absorbance at different times)

$$\ln(A0/At) = KDPBF \times t \quad (1)$$

The absorption rate of photos by photo sensitizers (K_{pho}) under irradiation was calculated by Eq.2 (P: the irradiating laser power (mV), A: absorbance, per cm, of the sensitizer at particular λ, λ: irradiation wavelength (nm), L: light path length of beam

(cm), V: sample volume (mL), 0.97: correction coefficient of reflected light from laser in air and on glass contact surface, 0.1197/λ: energy of 1 mol photo).

$$Kpho = \frac{0.97 \times P \times (1 - 10 - A \times L)}{(0.1197/\lambda) \times V} \times 100\% \quad (2)$$

$^1O_2$ quantum yields Φ is proportional to the rate of the target's disappearance to the rate of absorption of the photos by the sensitizers, K_{DPBF} to K_{pho} (K_{DPBF} /K_{pho}). As the value of the Φ_{ZnPc} is known, Φ_{ICG} can be calculated from Eq.3, and $\Phi_{Cu@mSiO_2\text{-}TD/ICG}$ can also be obtained with the same methods.

$$\frac{\Phi ICG}{\Phi ZnPc} = \frac{KDPBF, ICG / Kpho, ICG}{KDPBF, ZnPc / Kpho, ZnPc} \quad (3)$$

The absorption intensity of DPBF at 410 nm reduced over time and the relationship between $\ln(A_0/A_t)$ and time was plotted (Fig. S8a). The slope $K_{DPBF, ICG}$ derived from linear fitting is 2.838×10^{-2} min^{-1}. Based on all the information above, the Φ_{ICG} was calculated as 0.31. Likewise, $\Phi_{Cu@mSiO_2\text{-}TD/ICG}$ was calculated as 0.24 (Fig. S8b).

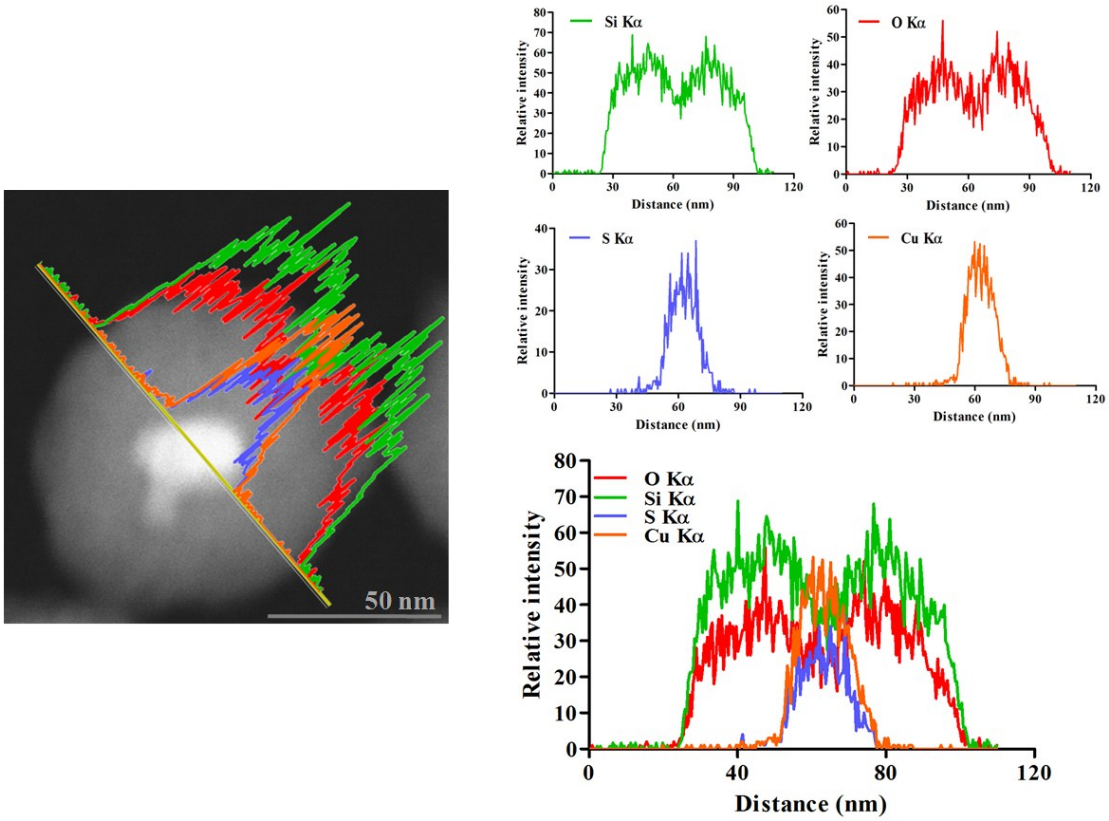

Fig. S1 EDX line scan with Si Kα signal, O Kα signal, S Kα signals and Cu Kα signals of the core-shell CuS@mSiO_2 nanoparticles.

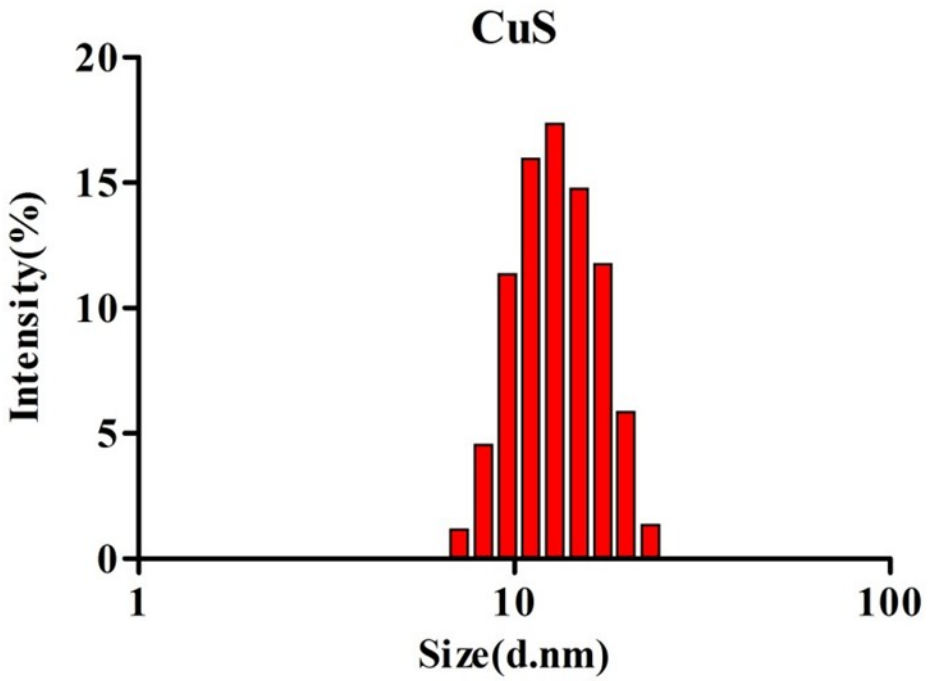

Fig. S2 Size distribution of CuS nanoparticles.

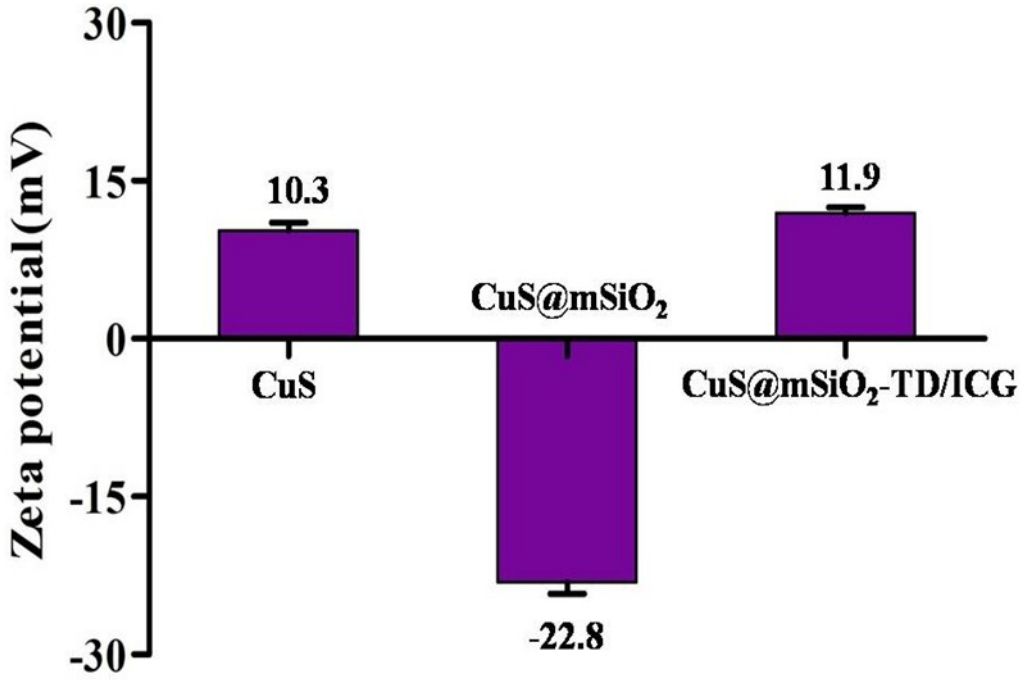

Fig. S3 Zeta potential of different formulations of CuS, CuS@mSiO$_2$, CuS@mSiO$_2$-TD/ICG, respectively.

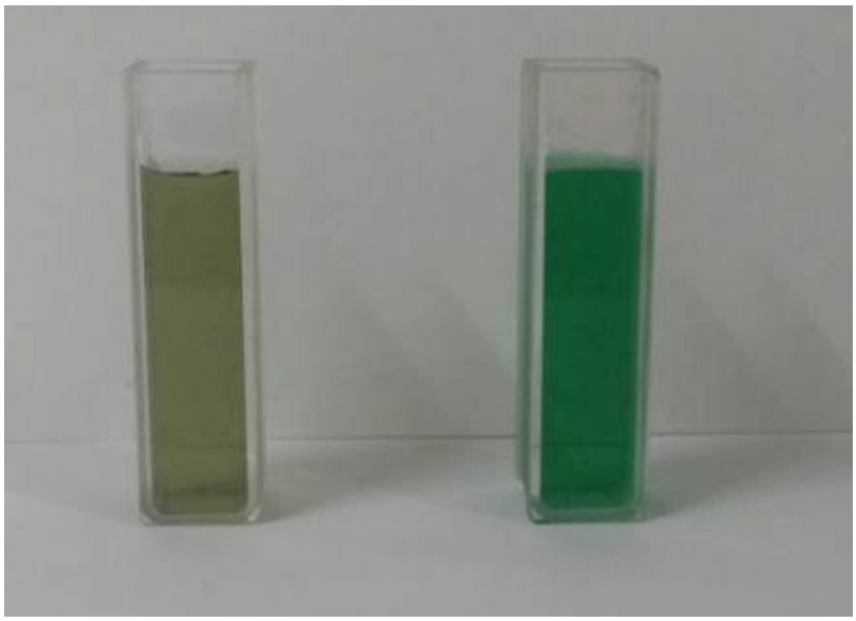

Fig. S4 Photographs of $CuS@mSiO_2$ (left) and $CuS@mSiO_2$-TD/ICG (left) and $CuS@mSiO_2$ (right), respectively, at an equivalent $CuS@mSiO_2$ concentration.

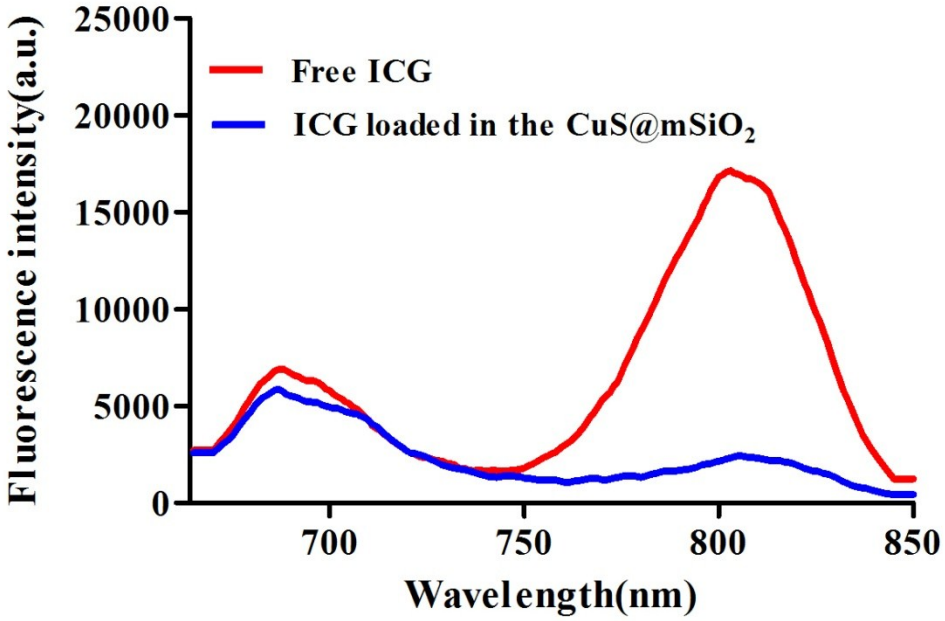

Fig. S5 Fluorescence emission spectra of free ICG and CuS@mSiO$_2$-TD/ICG (Ex: 650 nm).

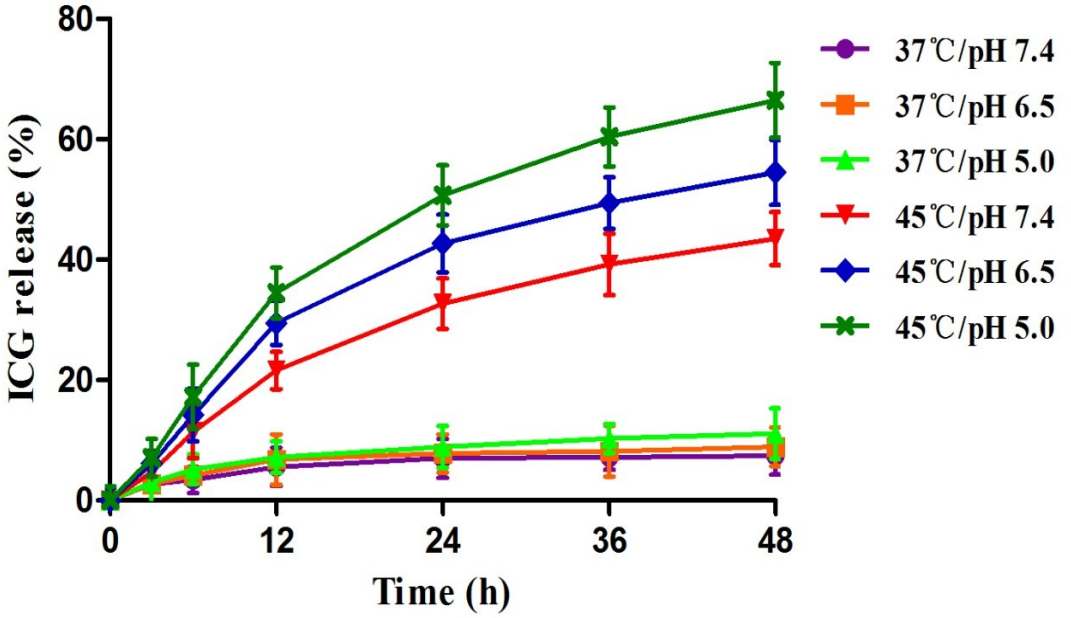

Fig. S6 Cumulative released ICG from the CuS@mSiO$_2$-TD/ICG under different pH values and temperatures.

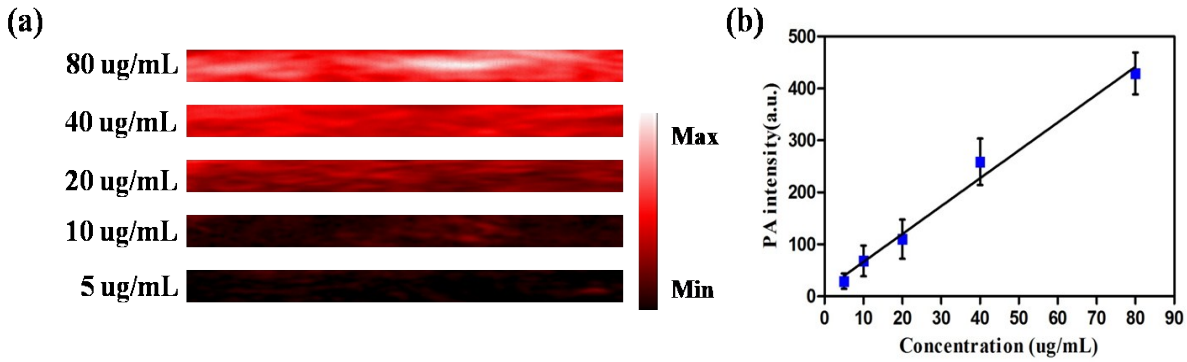

Fig. S7 (a) *In vitro* PA images of CuS@mSiO_2-TD/ICG aqueous solutions with increasing concentrations of ICG. (b) Linear relationship between PA intensity and ICG concentrations in CuS@mSiO_2-TD/ICG nanoparticles aqueous solutions.

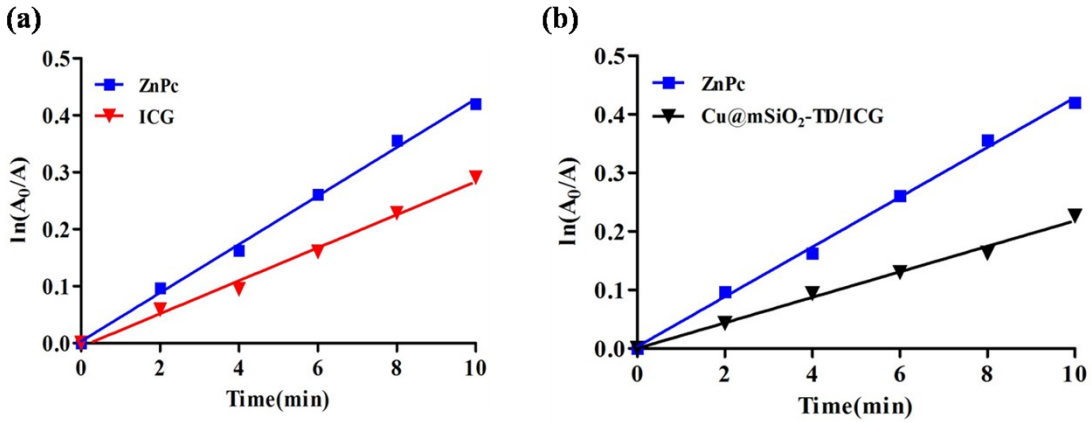

Fig. S8 (a) Plots of $\ln(A_0/A_t)$~t for the photobleaching of DPBF by ZnPc (λ=670 nm), ICG (λ=808 nm). (b) Plots of $\ln(A_0/A_t)$~t for the photobleaching of DPBF by ZnPc (λ=670 nm) and CuS@mSiO_2-TD/ICG (λ=808 nm).

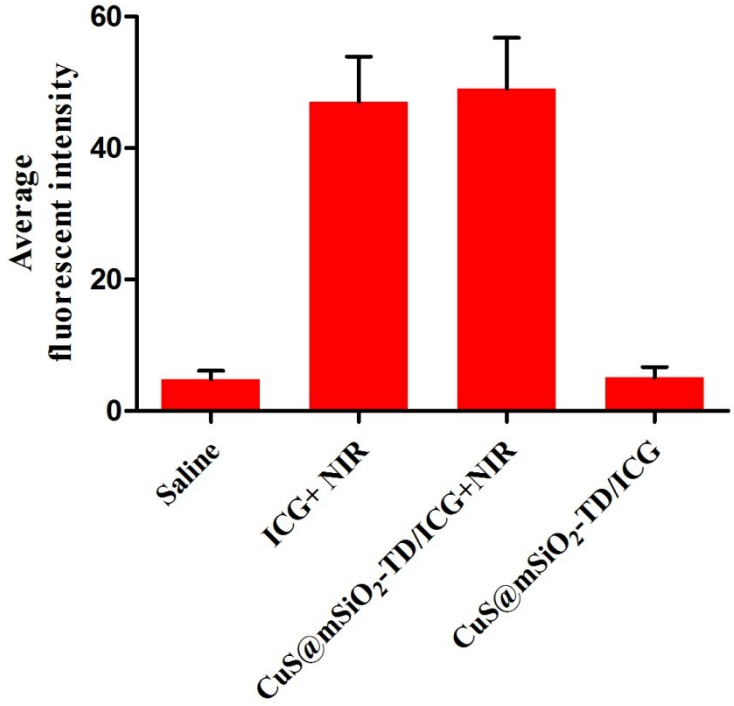

Fig. S9 The quantitative ROS generation analyses of different formulations (Saline, free ICG, CuS@mSiO$_2$ and CuS@mSiO$_2$-TD/ICG, respectively). The data were shown as mean ± SD (n = 3).

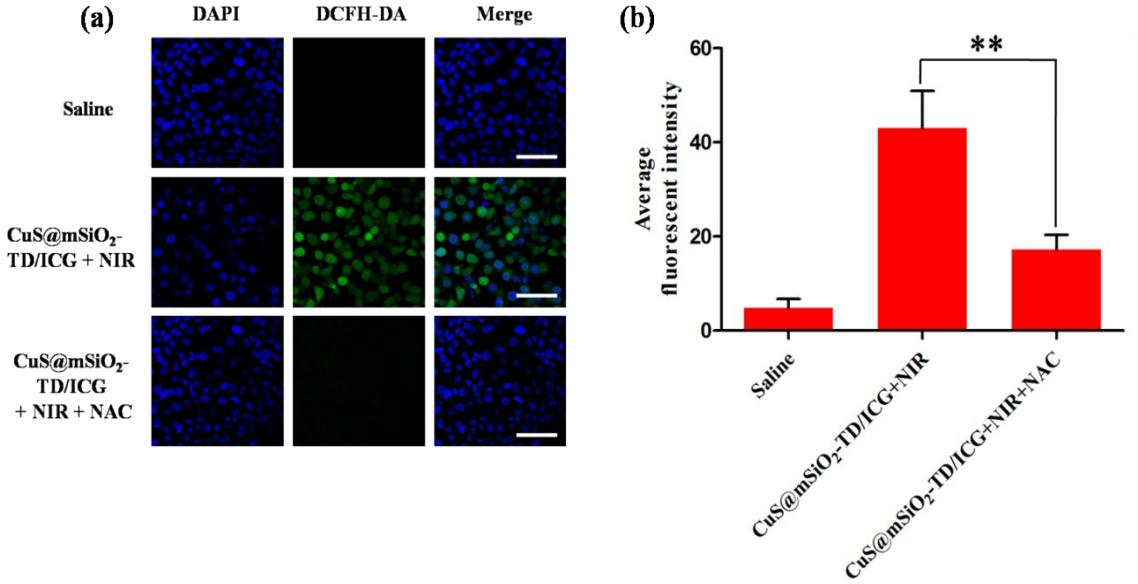

Fig. S10 (a) CLSM images of 4T1 cells treated with saline and CuS@mSiO$_2$-TD/ICG+NIR in the presence and absence of NAC. NIR laser irradiation at 808 nm (1.5 W/cm^2) for 5 min. Scale bars: 100 μm. (b) The quantitative analysis of the ROS generation of 4T1 cells treated with saline and CuS@mSiO$_2$-TD/ICG+NIR in the presence and absence of NAC. The data were shown as mean ± SD (n = 3).

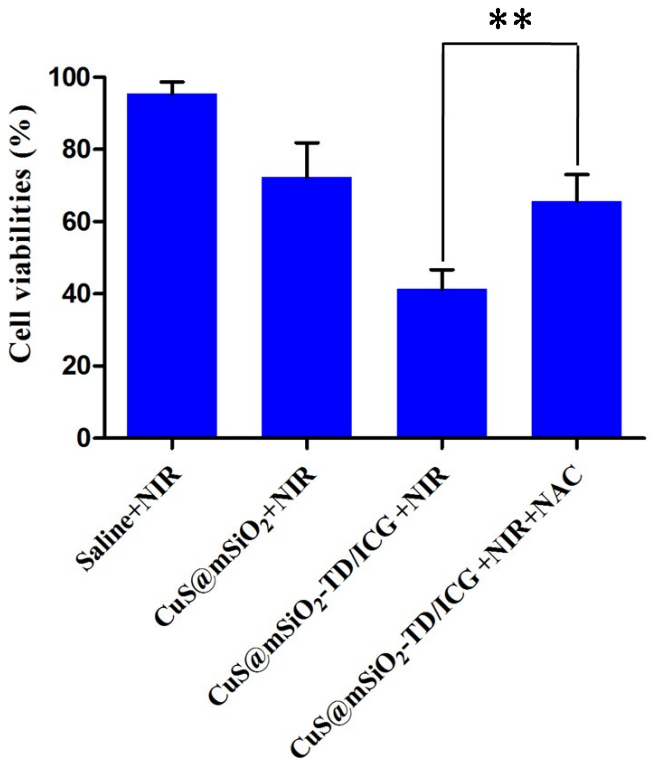

Fig. S11 Cell viability of 4T1 cells treated with saline, CuS@mSiO$_2$, CuS@mSiO$_2$-TD/ICG and CuS@mSiO$_2$-TD/ICG+NAC under laser irradiation (808 nm, 1.5 W/cm^2, 5 min). The data were shown as mean ± SD (n = 3).

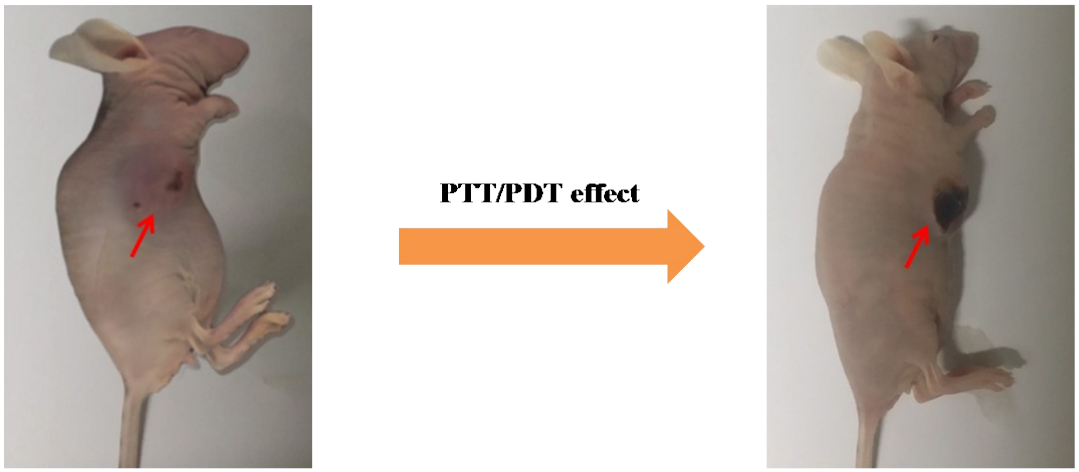

Fig. S12 Representative photos of CuS@mSiO_2-TD/ICG injected mouse at day 0 before PTT/PDT treatment and at day 15 after treatment.

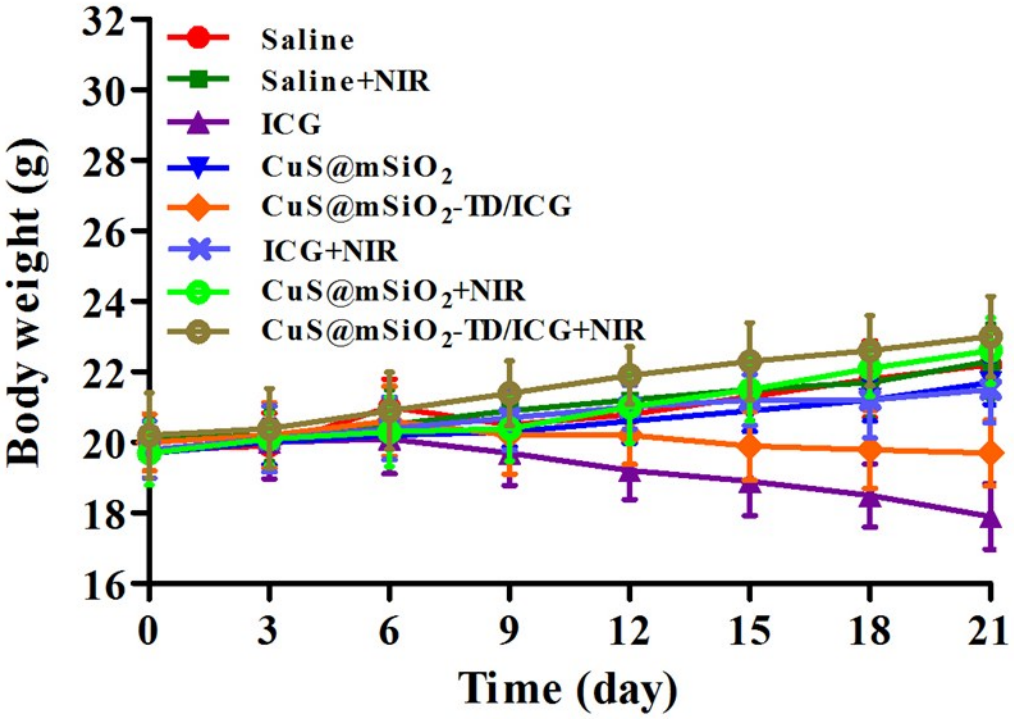

Fig. S13 Body weights of different treatment groups.

Ref:

1. W. Feng, X Zhou, W Nie, L Chen, K Qiu, Y Zhang and C He. *ACS Appl. Mater. Interfaces*, 2015, 7, 4354-4367.
2. Z. Jiang, T. Yang, M. Liu, Y. Hu and J. Wang. *Biosensors and bioelectronics*, 2014, **53**, 340-345.
3. A. Ogunsipe and T. Nyokong, *Journal of photochemistry and photobiology A: chemistry*, 2005, **173**, 211–220.
4. X. Xu, J. Wang, Z. Li, W. Yan, H. Chi, W. Chen, S. Zhuo and N. Chen, *Chinese Journal of Inorganic Chemistry*, 2011, **27**, 877-885.
5. H. Shinohara, O. Tsaryova, G. Schnurpfeil and D. Wohrle, *ournal of photochemistry and photobiology A: chemistry*, 2006, **184**, 50–57.